INVESTIGATIONS OF NEAR-ZONE DOPPLER EFFECTS

Thesis by

Dale Austen Prouty

In Partial Fulfillment of the Requirements

for the Degree of

Doctor of Philosophy

California Institute of Technology

Pasadena, California

1982

(Submitted May 24, 1982)

ACKNOWLEDGEMENTS

I would like first to thank my advisor, Professor Papas, for bearing with me through a rather protracted graduate study, for always adding encouragement in this slow process, and finally for always showing a great willingness to help me finish. Next, I thank Hughes Aircraft Company for extending my fellowship repeated times and for bringing my life into an exciting world I would have otherwise never known. I would also like to thank Janice Tucker for typing my thesis in the waning moments of the 1982 academic year, and finally, but not least, countless other friends and relatives who continually pushed me forward through good times and bad.

ABSTRACT

Far away from an electromagnetic source the normal Doppler shifts in frequency occur — a red shift for receding and a blue shift for approaching. As indicated by previous work with an infinitesimal dipole, different frequency shifts occur when the source and observer move closer together, into the near-zone. These "near-zone Doppler effects" are investigated for general sources and subsequently two specific examples are presented.

The general results show that near-zone shifts are similar to far-zone shifts, but the local phase velocity must be used, i.e. $\omega' \simeq \omega(1 \pm \frac{v}{v_{ph}})$. In the far zone the phase velocity is the speed of light; in the near zone it differs. Fundamentally, the distance between surfaces of constant phase in the near zone is changed. The surfaces of constant phase for the waves are no longer spherical, but more ellipsoidal or spheroidal, so that a moving observer sees a different frequency shift.

Two specific examples are presented to indicate the actual magnitude of near-zone effects. The examples include a prolate spheroidal antenna and a circular aperture.

Once the magnitude of the effects is determined, the measurability of near-zone Doppler effects is discussed. The investigation concentrates on Fresnel zone effects due to the measurement problem.

Finally, it is shown that for an electrically large wire antenna (the spheroidal example) near-zone Doppler effects are measurable.

TABLE OF CONTENTS

INTRODUCTION

A red shift when receding, a blue shift when approaching — such are the well-known Doppler shifts or Doppler effects [1] on electromagnetic radiation in free-space due to relative motion of the source and observer. Interestingly, these well-known shifts do not always occur as expected. Frank [2] and K. S. H. Lee [3] have shown that in some dispersive media an "inverse Doppler effect" can occur where a red shift is observed when approaching. Papas, Engheta, and Mickelson [4] have shown that the near-zone field of a free-space dipole also presents similar inverse shifts. In addition, it was shown that the near-zone effects could provide range and polarization information, as well as velocity, by measuring the various field components separately. The purpose of this dissertation is to further investigate these effects.

This investigation, including the general discussion of measurability, provides insight into the practical application of these results. Maxwell's equations [5] will be used to show that many sources have near-zone Doppler effects which are not identical to far field effects. Some will be shown simply to go from a far field blue shift through zero to a far field red shift. Others will be shown to have "inverse" effects in the near-zone. Fields of some specific antennas that can be computed exactly or with accurate near-zone approximations will be used to show the general existence and spatial extent of these effects.

The spatial extent relates to the measurability or practical application of the results. A detailed description of the problems involved in measuring the effects will help point out the source features required for producing measurable results.

The various chapters of this dissertation will describe the investigation of the near-zone and inverse Doppler effects. Chapter 1 presents general results applicable to any source, (derived directly from the covariance of Maxwell's equations under Lorentz transformation). Chapter 2 reviews the results of the dipole and goes on to present results for a prolate spheroidal antenna and a circular aperture. Chapter 3 discusses the measurability of the effects and implications of the results of Chapters 1 and 2. This discussion leads to an example of a source with measurable effects. Chapter 4 provides a final summary and conclusions of this work.

CHAPTER 1. GENERAL BACKGROUND AND RESULTS

Many near-zone calculations have been made in the past [6], but the basic purpose was to obtain amplitude information, usually to infer far-zone gain patterns from near-zone measurements. The near-zone Doppler effects, in contrast, are derived from the phase of the fields. We can, however, apply much of the same nomenclature and many of the analytic or calculation techniques used in this previous work to the phase problem.

The theory applicable to the near-zone Doppler effects involves Lorentz transformations and appropriate approximations to the field equations. The phase of the transformed field components will be used to formulate a frequency shift function encompassing the near-zone Doppler shift. A discussion of general near-zone approximations based on previous work will indicate methods to be used in the investigation of our phase problem. The general background material of this chapter will not only provide a common framework for discussion of the specific examples of the next chapter, but will also indicate the specific types of antennas (or sources) to consider in those examples.

Now, back to the Lorentz transformations ... Consider the inertial frames of the source and observer. Let K be the source frame, K' be the observer frame, and $\bar{v}$ be the relative velocity of K' with respect to K. Also, let the coordinate frames be similarly oriented and coincident at $t = t' = 0$ as shown in Figure 1. The field equations in the observer frame are then [7]:

Figure 1 Source and Observer Reference Frames

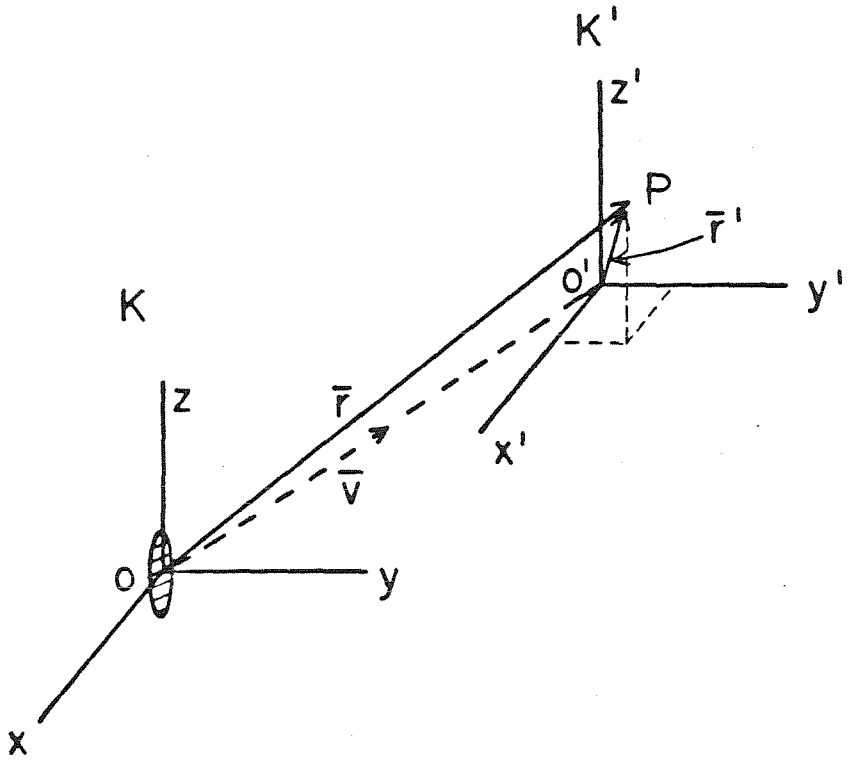

K is the source frame (O is the origin)

K' is the observer frame (O' is the origin)

$\bar{v}$ is the relative velocity

P is the point of observation (fixed in K')

$\bar{r}$ is the source vector to P

$\bar{r}'$ is the observer vector to P

Note: If $\bar{r}' = 0$, i.e. P = O', $\hat{r} = \begin{cases} \hat{v} & \text{for } t > 0 \\ -\hat{v} & \text{for } t < 0 \end{cases}$

where $\hat{r}$, $\hat{v}$ are unit vectors along $\bar{r}$, $\bar{v}$ respectively.

$$\overline{E}' = \gamma(\overline{E} + \overline{\beta} \times c\overline{B}) + (1-\gamma) \frac{\overline{E} \cdot \overline{\beta}}{\beta^2} \overline{\beta} \tag{1}$$

$$c\overline{B}' = \gamma (c\overline{B} - \overline{\beta} \times \overline{E}) + (1-\gamma) \frac{c\overline{B} \cdot \overline{\beta}}{\beta^2} \overline{\beta} \tag{2}$$

where $\overline{E}$, $\overline{B}$ are the electric and magnetic fields of the source, $\overline{\beta}$ is the normalized relative velocity (i.e. $\overline{\beta} = \overline{v}/c$, where c is the speed of light), and $\gamma \equiv (1 - \beta^2)^{-1/2}$. The coordinate transformations may similarly be written [7]:

$$\overline{r} = \overline{r}' + \gamma\overline{\beta}\, ct' + (\gamma-1) \frac{\overline{r}' \cdot \overline{\beta}}{\beta^2} \overline{\beta} \tag{3}$$

$$ct = \gamma(ct' + \overline{r}' \cdot \overline{\beta}) \tag{4}$$

where the equations are for the source frame coordinates in terms of those of the observer. This will be useful later. We will return to these equations during the derivation of the Doppler effect.

The field function important for the Doppler effect is, as already mentioned, the phase, or more precisely, the frequency. The frequency will be defined here as a time derivative of the phase (i.e. $\omega' \equiv - \frac{d}{dt'}\phi$). The phase ϕ must now be determined so that the Doppler effect may be investigated.

In the observer frame K', a component of the field along the $\hat{n}'$ direction may be written:

$$\hat{n}' \cdot \bar{E}' = (R + iI)e^{-i\omega t} \tag{5}$$

where R and I are the real and imaginary parts respectively, and it is assumed that the source has harmonic time dependence. This may also be written

$$\hat{n}' \cdot \bar{E}' = A \exp[i(\tan^{-1}(\frac{I}{R}) - \omega t)] \tag{6}$$

where $A = (R^2 + I^2)^{1/2}$. The phase is

$$\phi = \theta - \omega t = \tan^{-1}(\frac{I}{R}) - \omega t \tag{7}$$

Note that we leave ϕ in source coordinates $\bar{r},t$; this will simplify the mathematics.

Now, the frequency measured by the observer is

$$\omega' \equiv - \frac{d}{dt'} (\theta - \omega t), \tag{8}$$

To evaluate ω', note:

$$\frac{d}{dt'} f(\bar{r},t) = \frac{dt}{dt'} \cdot \frac{\partial f}{\partial t} + \frac{d\bar{r}}{dt'} \cdot \nabla f \tag{9}$$

Using equations (3) and (4), we obtain

$$\frac{d}{dt'} f(\bar{r},t) = \gamma \frac{\partial f}{\partial t} + \gamma c\bar{\beta} \cdot \nabla f \tag{10}$$

thus

$$\omega' = \gamma\omega[1 - \frac{\bar{\beta} \cdot \nabla}{k} \theta] \tag{11}$$

where $\omega = kc$. To maintain consistency with Papas, et al.[4], we write

this as

$$\omega' = \gamma\omega[1 - \beta\eta] \tag{12}$$

where

$$\eta = \frac{\hat{\beta} \cdot \nabla}{k}\theta \tag{13}$$

and $\hat{\beta} = \frac{\bar{\beta}}{\beta}$.

Before proceeding, we should discuss this function "η" to see some fundamental things about near-zone Doppler effects. First, we will discuss the phase velocity in both the observer and source frames; then, we will return to our definition of frequency. Recall the definition of phase velocity [8]:

$$v_{ph} \equiv \frac{\omega}{\frac{\partial\phi}{\partial r}} \quad \text{, or more generally,}$$

$$v_{ph} \equiv \frac{\omega}{\hat{e} \cdot \nabla\phi} \tag{14}$$

where $\hat{e}$ is a unit vector along the direction of measurement. Since, in our case we measure only at the origin in the observer frame, we do not measure phase velocity, but rather the change in time of the received phase, i.e. $\omega' = \frac{-d\phi}{dt'}$. The phase velocity of the source frame, however, is measured and has interesting properties in the near-zone. There $v_{ph} = \frac{\omega}{\hat{e} \cdot \nabla\phi}$. If we choose $\hat{e} = \hat{\beta}$, i.e. the direction along which motion is eventually to be considered,

$$v_{ph} = \frac{\omega}{\hat{\beta} \cdot \nabla\phi} \quad . \tag{15}$$

Thus,

$$\frac{c}{v_{ph}} = \frac{\hat{\beta} \cdot \nabla\phi}{\omega / c} = \hat{\beta} \cdot \frac{\nabla}{k} (\theta - \omega t) = \hat{\beta} \cdot \frac{\nabla\theta}{k} \tag{16}$$

so,

$$\eta = \frac{\hat{\beta} \cdot \nabla}{k} \theta = \frac{c}{v_{ph}} \tag{17}$$

or more strikingly,

$$\omega' = \gamma \omega \left(1 - \frac{v}{v_{ph}}\right) . \tag{18}$$

The near-zone Doppler effects are similar to far-zone Doppler effects, except we must replace the far-zone phase velocity, c, by the near-zone phase velocity, which varies as a function of position.

Alternatively, the function $\eta = \frac{c}{v_{ph}}$ could be thought of as representing an index of refraction for a dielectric (or permeable media for magnetic fields) that varies with position. The equivalent dielectric is

$$\varepsilon(\bar{r}) = \varepsilon_0 \eta^2(\bar{r}) \quad . \tag{19}$$

This interpretation may be somewhat artificial, although knowledge of waves in dielectric media might add some insight into the process. Probably more important is the fact that variations in dielectric "constant" of the same order as these shifts cannot be distinguished. Thus shifts must be larger than any equivalent local dielectric variations in the medium in which measurements are being made.

The far-zone "plane waves" (actually spherical surfaces) simply no longer exist in the near field. When the source is near, the waves

are distorted much as they might be in certain dielectric media. Also, the first features of the source to be noticed in the new waves would be the approximate size or maximum linear dimension, i.e. some crude information about the source itself. This idea will be borne out in the pages that follow. We will return to these ideas after we do some further calculations of η to see what forms it actually takes.

To obtain the variations in η, we must determine the phase of the fields. This can be done directly, by evaluating θ as $\tan^{-1}(\frac{I}{R})$, and then taking the derivatives; or we can use the fields directly. This can be seen as follows:

With $\theta = \tan^{-1}(\frac{I}{R})$ and by using equation (13)

$$\eta = \frac{\hat{\beta} \cdot \nabla}{k} \theta = \frac{\hat{\beta}}{k} \cdot \frac{(\nabla I)R - (\nabla R)I}{I^2 + R^2} \quad . \tag{20}$$

By ignoring the $e^{-i\omega t}$ time dependence, we can substitute

$$I = \frac{\hat{n}' \cdot \bar{E}' - \hat{n}' \cdot \bar{E}'^*}{2i} \quad \text{and} \quad R = \frac{\hat{n}' \cdot \bar{E}' + \hat{n}' \cdot \bar{E}'^*}{2} \tag{21}$$

where the asterisk represents complex conjugation. Eta may then be written

$$\eta = \text{Imag} \left\{ \frac{\frac{\hat{\beta} \cdot \nabla}{k} (\hat{n}' \cdot \bar{E}')}{\hat{n}' \cdot \bar{E}'} \right\} , \tag{22}$$

where Imag { } indicates the imaginary part. Either equation (13) or this one may be used to evaluate η.

Recall that in the equation for the frequency (12), the shift is already first order in β. When considering small velocities, and retaining frequency shifts only to first order in β, approximations may be made as follows:

$$\begin{aligned} \gamma &\simeq 1 \\ \bar{E}' &\simeq \bar{E} \\ \bar{B}' &\simeq \bar{B} \\ \hat{n}' &\simeq \hat{n} \end{aligned} \tag{23}$$

so,

$$\eta \simeq \text{Imag}\left\{ \frac{\frac{\hat{\beta} \cdot \nabla}{k} (\hat{n} \cdot \bar{E})}{(\hat{n} \cdot \bar{E})} \right\} . \tag{24}$$

A similar equation can be written for the components of $\bar{B}$.

A brief discussion of η is worthwhile to point out the expected values of this frequency shift function in the far-zone and for inverse effects. As the source approaches from far away $\eta = -1$, that is $\omega' = \omega(1+\beta)$. There is a blue shift. As it recedes $\eta = +1$, $\omega' \simeq \omega(1-\beta)$, and there is a red shift. If, as the source approaches, η changes from negative to positive prior to passing the observer, an inverse Doppler effect has occurred. This can only occur in the near-zone; Doppler effects in the far zone are well known and are the two cases $\eta = \pm 1$ just presented. Even if an inverse effect does not

occur, the near-zone value of η may deviate from ± 1. In fact, the details of the frequency shifts, represented by η, will emphasize this case throughout this work.

Now that we have derived the near-zone equations in terms of the fields, it is necessary to explicitly describe the source fields. The field components for general source distributions will first be written exactly and subsequently appropriate approximations can be made. Two types of sources will be considered — current distributions and apertures. For current sources the fields may be written (see Appendix I)

$$\bar{E} = i\mu\omega k \int_J \frac{e^{ikR}}{4\pi kR} \left\{ \bar{\bar{u}}\left[\frac{k^2R^2+ikR-1}{k^2R^2}\right] + \hat{R}\hat{R}\left[\frac{-k^2R^2+3ikR+3}{k^2R^2}\right] \right\} \cdot \bar{J}d\bar{r}'' e^{-i\omega t} \qquad (25)$$

$$c\bar{B} = \mu\omega k \int_J \frac{e^{ikR}}{4\pi kR} \left[\frac{ikR-1}{kR}\right] \hat{R} \times \bar{J}d\bar{r}'' \, e^{-i\omega t} \qquad (26)$$

where $\bar{J}$ is the current density of the source, and $R = |\bar{r}-\bar{r}''|$, $\hat{R} = (\bar{r}-\bar{r}'')/|\bar{r}-\bar{r}''|$. For aperture distributions the fields may be written (see Appendix II)

$$\bar{E} = 2k^2 \, e^{-i\omega t} \int_A \hat{R} \times (\hat{a} \times \bar{E}) \frac{e^{ikR}}{4\pi kR} \left(\frac{ikR-1}{kR}\right) d\bar{r}'' \qquad (27)$$

$$c\bar{B} = 2k^2 \, e^{-i\omega t} \int_A \hat{R} \times (\hat{a} \times c\bar{B}) \frac{e^{ikR}}{4\pi kR} \left(\frac{ikR-1}{kR}\right) d\bar{r}'' \qquad (28)$$

where $\overline{E}$ and $\overline{B}$ inside the integrals represent the total fields in the aperture; $\hat{a}$ is the normal to the aperture pointing into the diffracted region.

Now that the exact field descriptions have been given, we will examine appropriate approximations. The results of previous near-zone work [9-11] indicate useful near-zone integral approximations. These results also aid in understanding what we might expect the spatial extent of the near-zone effects to be. Several good discussions of the near-zone and its limited extent are found in the above cited literature. The essence of these discussions will be summarized here.

The fields of a source are commonly divided into three regions — the reactive near field, the radiating near field and the far field. The reactive near field commonly extends at most a few wavelengths from the source. It includes field terms which decrease faster than $(kr)^{-1}$, and, in general, no approximations can be made to the integral equations. Beyond this distance the radiating fields predominate. The radiating near field extends for a distance of approximately $2D^2/\lambda$, where D is the maximum linear dimension of the source and λ is the wavelength. In this region the gain pattern varies as a function of distance from the source, and integral approximations similar to the Fresnel approximations are commonly applied. The radiating far field extends to infinity. In this region the gain pattern does not vary as a function of distance and the Fraunhofer or similar approximations are usually made.

Our investigation of near-zone effects concentrates primarily on the radiating near field region. This is where integral approximations are useful and somewhat well understood. As just mentioned, this region is commonly assumed to extend a distance $\frac{2D^2}{\lambda}$. This limit is derived from the phase approximations made in the integral equations, i.e. in $e^{ik|\bar{r}-\bar{r}''|}$. If the phase contributions at $\bar{r}$ from points near the source center ($\bar{r}'' \simeq 0$) and the source boundary ($\bar{r}'' = D/2$) differ by more than $\frac{2\pi}{16} = 22.5^0$, the Fresnel approximation must be used. This is equivalent to saying the Fresnel approximation must be used if the relative path lengths differ by more than $\lambda/16$. If a similar criterion is applied to the subsequent term in the phase expansion, an inner boundary of the Fresnel zone may be obtained — $R = \frac{D}{2}\left(\frac{D}{\lambda}\right)^{1/3}$. Similar criteria may be imposed on the relative magnitudes of amplitude terms. The limits of our region of interest are thus outlined and are shown in Figure 2.

This discussion, as presented in Figure 2, is meant as a guide to give us understanding; it is not a presentation of definitive limits for the radiating near field for all possible antennas. For example, as will be discussed further, supergain antennas may extend the Fresnel zone much beyond $2D^2/\lambda$. An example cited in Hansen [11] describes noticeable effects to $22D^2/\lambda$. Also the Fresnel amplitude approximations may not be valid at some distance from the source greater than that depicted. In either case we will use these region boundaries to give

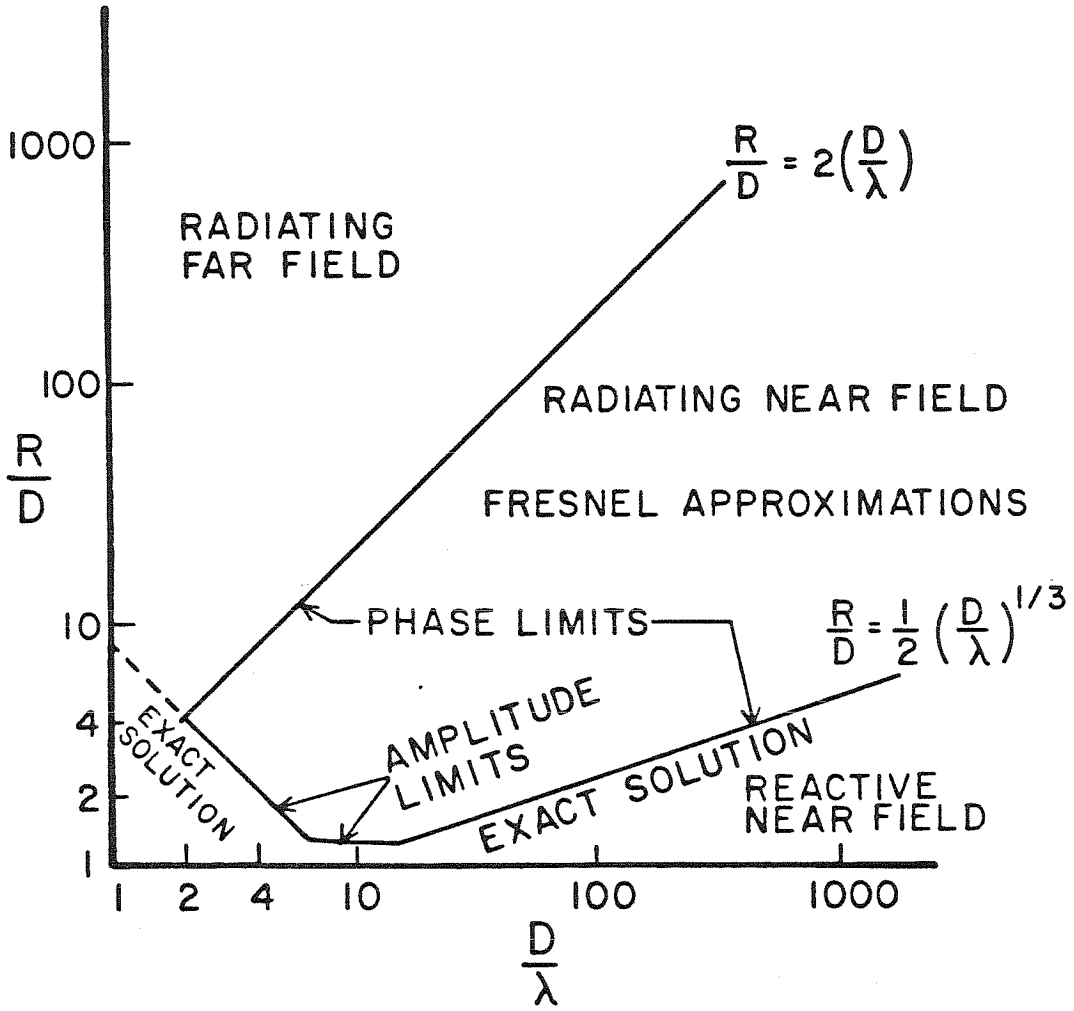

Figure 2 Spatial Extent of Approximation Regions*

* This is a compilation of various works [10-11], each of which makes similar but slightly different assumptions about the phase and amplitude approximations of the Fresnel zone.

us a starting point. The implications of these boundaries for the near-zone Doppler effects include a requirement for electrically large or high gain antennas. It is obvious that for measurability and practical usefulness we would like the near-zone extent to be as far reaching as possible. If we use the $2D^2/\lambda$ criterion as the crude boundary of the near-zone, the spatial extent of near-zone effects could only be increased by making D larger relative to λ. We would also like to be as far from the source as possible, i.e. we want $\frac{R}{D} \sim \frac{2D}{\lambda}$ to be large. This means we need electrically large antennas, or, alternatively, since the gain of a transmitting antenna is roughly proportional to $\frac{D^2}{\lambda^2}$, we could use high gain antennas. Supergain antennas might be appropriate. These antennas provide higher directivity than common antennas, i.e. supergain, and might provide near-zone effects even further from the source. There are, however, serious practical limitations in the use of supergain antennas. The problems in practical application become evident when we realize that tolerances of the current or aperture distribution on the order of 1 part in 10^{-10} may be required to increase directivity by a factor of 16 [11] and may or may not increase the spatial extent of the near-zone Doppler effects. Since the purpose here is to investigate the generality of the near-zone effects, and not to find the best source available (even with practical limitations) we will not delve into these antennas further.

Next, we will make a series expansion of the fields to obtain the Fresnel approximation showing the relative magnitudes of the frequency shifts as the observer first measures the near-zone fields of the source. We proceed by making a series expansion of the field equations (25-28). The electric field of the aperture antenna will be used in an example of this expansion.

$$\hat{n} \cdot \bar{E} = \int \sum_{n=1}^{\infty} \frac{A_n(\theta,\phi,\theta'',\phi'',r'')}{(kr)^n} e^{ikR} \; \hat{n} \cdot \bar{E}''(\bar{r}'')d\bar{r}'' \qquad (29)$$

where only the amplitude terms are expanded. For the Fresnel zone, only A_1 is kept and only up to quadratic terms are kept in the phase. Thus

$$\hat{n} \cdot \bar{E} \simeq \frac{A_1}{kr} e^{i(kr-\omega t)} \int e^{i\frac{k^2 r''^2}{2kr}} \; \hat{n} \cdot \bar{E}(\bar{r}'')d\bar{r}'' \qquad (30)$$

Now, to calculate η, recall

$$\eta \simeq \text{Imag} \left\{ \frac{\frac{\hat{\beta} \cdot \nabla}{k} (\hat{n} \cdot \bar{E})}{\hat{n} \cdot \bar{E}} \right\}.$$

We will assume that measurement is made at the origin of the observer frame K'; then, as shown in Figure 1, $\hat{\beta}$ is proportional to $\hat{r}$, i.e. $\hat{\beta} = \hat{r}s$ where $s = \begin{cases} +1 & t > 0 \\ -1 & t < 0 \end{cases}$. This will simplify the results by avoiding confusion with aberration effects [7]. So

$$\eta = s \ \text{Imag} \left\{ \frac{\frac{\partial}{\partial kr} (\hat{n} \cdot \bar{E})}{\hat{n} \cdot \bar{E}} \right\} . \tag{31}$$

Now, applying the derivative to the series expansion (29) for the aperture case yields

$$\eta = s \left(1 - \frac{1}{k^2 r^2} \text{Real} \left\{ \frac{\int_A \frac{1}{2} k^2 r''^2 \, e^{i \frac{k^2 r''^2}{2kr}} (\hat{n} \cdot \bar{E}'') d\bar{r}''}{\int_A e^{i \frac{k^2 r''^2}{2kr}} (\hat{n} \cdot \bar{E}'') d\bar{r}''} \right\} + \ldots \right) \tag{32}$$

where Fresnel approximations have been used and $\bar{E}''$ is the aperture field. (Only first order amplitude terms and quadratic phase terms were kept). If the integral of the numerator were large compared with the denominator the assumption that only first order amplitude terms need to be kept would break down. This, and other details, are found in Appendix II.

Similar expansions for the other field equations, as shown in the Appendices, lead to the same result for the appropriate field component. For the current source electric field

$$\eta \simeq s \left(1 - \frac{1}{k^2 r^2} \text{Real} \left\{ \frac{\int_J \frac{1}{2} k^2 r''^2 \, e^{i \frac{k^2 r''^2}{2kr}} (\hat{n} \cdot \bar{J}) d\bar{r}''}{\int_J e^{i \frac{k^2 r''^2}{2kr}} (\hat{n} \cdot \bar{J}) d\bar{r}''} \right\} + \ldots \right) \tag{33}$$

Note that if no radiating field component exists, for instance in the radial direction, the Fresnel approximation, which gives the radiating near field, is useless. Second and higher order amplitude terms of the reactive near field must be included in order to measure fields and frequency shifts since no Fresnel zone field exists. It is thus apparent that generally the only field components with appreciable shifts in the Fresnel zone are the same far field radiating components.

The results of equations (32) and (33) (including comments from the Appendices on the magnitude of the shifts in the Fresnel zone) indicate that no "inverse" Doppler effects are generally present in the Fresnel zone. For "inverse" effects, we must then look into the reactive near field; the measurability then comes into question, as discussed in Chapter 3, since only a few wavelengths are available over which to measure (resolve) the shift. The much more general near-zone frequency shifts are fractional corrections to the far-zone values, and in fact, were shown to be

$$|\partial\omega| \simeq (\frac{v}{v_{ph}})\omega$$

A simple example may help to give insight into the near-zone effects. If a linear source of length D is radiating electromagnetic waves, we might expect surfaces of constant phase in the outer region of the near zone to not be quite spherical, but more elliptical, or rather spheroidal with the curvature related to D. The wavelength

(distance between surfaces of constant phase differing by 2π) of far zone radiation might be slightly different from that of the near zone. (The near-zone distance will be shown to be larger). Now, with a moving source, the frequency of the waves as measured by the observer will include a Doppler shift just as in the far-zone case; however, since the distance between surfaces of constant phase is larger in the near zone than the far zone the actual shift will be reduced for both approaching and receding sources.

Specific examples of various antennas and source distributions are given in the next chapter. The general results of this chapter will be used to choose the specific examples to be presented, and the results for the examples will be demonstrated in the limits of the Fresnel or similar approximations.

CHAPTER 2 - SPECIFIC EXAMPLES

The purpose of this chapter is first to review the importance of the previous near-zone Doppler work for the case of an infinitesimal dipole [4] and gain some insight from it, as well as the results of the last chapter. This insight will then lead us to investigations of two antennas — an electrically large prolate spheroidal antenna and a large aperture.

A. Review

The previous work on an infinitesimal dipole showed three interesting results.

(1) Doppler effects, different from the far-zone effects, were present in the near-zone of an electromagnetic source and possibly in many or all such sources.

(2) The near-zone effects differed depending upon which component of the electric field or magnetic field was measured.

(3) The near-zone shifts depended on the distance between the source and observer, thus giving information about range, in addition to the normal far-zone velocity information.

This chapter will investigate further these results for two specific source types.

Although the exact details of measurability are left to Chapter 3, it is evident from the previous discussion of Chapter 1 that the

infinitesimal dipole is not a particularly good candidate for measurable effects far from the source. This dipole is essentially an approximation to a real source where $\frac{D}{\lambda} << 1$; it simply does not fulfill the electrically large criterion. It remains then to find sources with fields that may be calculated exactly or with accurate near-zone approximations, but that are electrically large or high gain.

Luckily, the prolate spheroidal antenna fields may be calculated exactly and circular aperture fields may be calculated accurately in the Fresnel zone. These two sources can both be electrically large. The resulting near-zone Doppler effects will be presented with appropriate limitations indicated.

B. Prolate Spheroidal ("Cigar-Shaped") Antenna

For a perfectly conducting prolate spheroidal antenna aligned with the z-axis and center-driven by an axially symmetric source field linearly polarized in a direction parallel to the axis [12]:

$$c\bar{B} = cB_{\phi}\hat{\phi}, \text{ and } \bar{E} = i\frac{\nabla}{k} \times c\bar{B} . \tag{34}$$

Prolate spheroidal coordinates are a convenient set to use to describe the fields, since in source free regions this coordinate system is one in which Maxwell's equation separate [13]. The coordinates are labeled (ξ,η,ϕ) and are somewhat similar to a normalized set of (r,θ,ϕ) since for large $r, (\xi,\eta,\phi) \rightarrow (\frac{r}{D/2}, \cos\theta, \phi)$ where D is

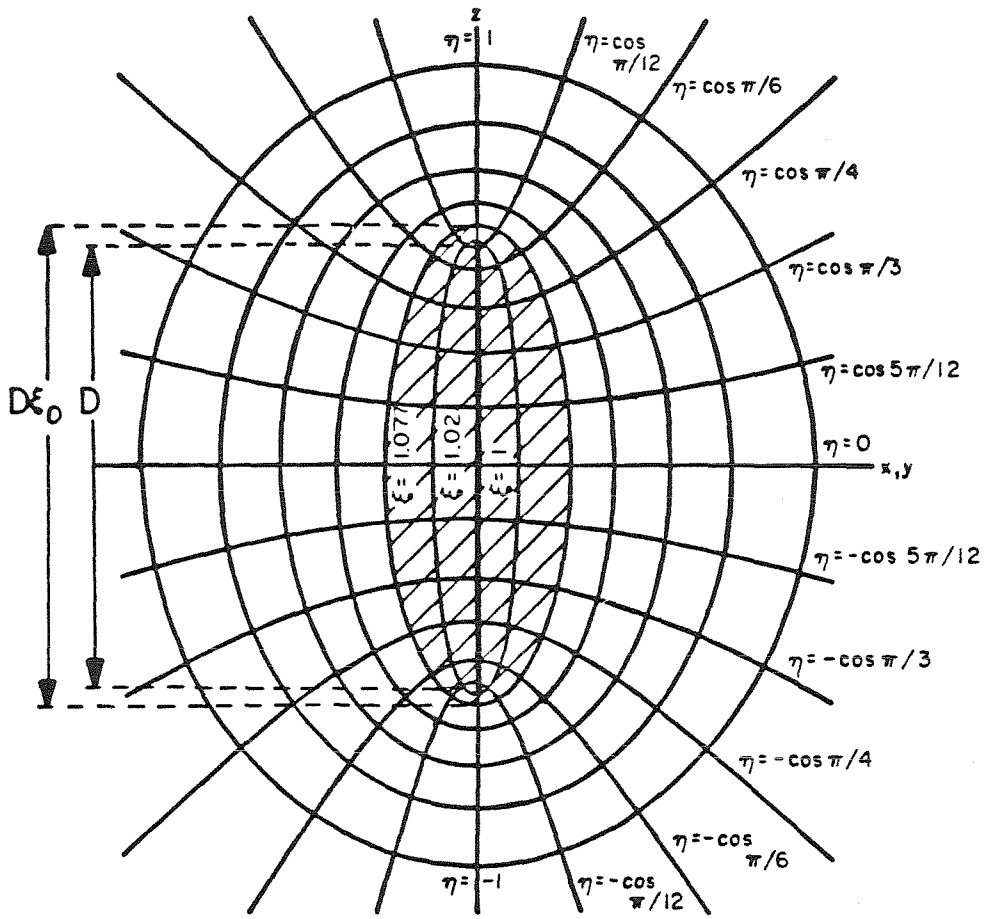

Figure 3 Prolate Spheroidal Coordinate System [14]

$$\left.\begin{matrix}\xi^2\\ \eta^2\end{matrix}\right\} = \frac{\left(\frac{r^2}{(D/2)^2} + 1\right) \pm \sqrt{\frac{r^4}{(D/2)^4} - 2\cos 2\theta \frac{r^2}{(D/2)^2} + 1}}{2}$$

$D_{ACTUAL} = \xi_o D$ is the actual antenna length

D is tne distance between foci

the approximate antenna length for narrow spheroids (see Figure 3). The magnetic field can be expanded in terms of the spheroidal functions as:

$$cB_\phi = \sum_{\ell=1}^{\infty} a_\ell \, S_{1,\ell}(c,\eta) \, R^{(3)}_{1,\ell}(c,\xi) e^{-i\omega t} \tag{35}$$

where a_ℓ are determined by boundary conditions and $c = kD/2$. $S_{1,\ell}$ and $R^{(3)}_{1,\ell}$ are the appropriate angular and radial prolate spheroidal wave functions, respectively. The notation followed here and many of the formulae used in derivations are from Flammer [14].

The electric field may be derived from

$$\bar{E} = i \frac{\nabla}{k} \times c\bar{B} \quad .$$

The resulting field is:

$$\bar{E} = \frac{ie^{-i\omega t}}{(k\,D/2)} \left\{ \sum_{\ell=1}^{\infty} a_\ell \left[\frac{-\eta}{(1-\eta^2)^{1/2}(\xi^2-\eta^2)^{1/2}} S_{1,\ell}(\eta) R^{(3)}_{1,\ell}(\xi) \right. \right.$$

$$+ \frac{(1-\eta^2)^{1/2}}{(\xi^2-\eta^2)^{1/2}} \frac{dS_{1,\ell}(\eta)}{d\eta} R^{(3)}_{1,\ell}(\xi) \Big] \hat{\xi} - \sum_{\ell=1}^{\infty} a_\ell \left[\frac{\xi}{(\xi^2-1)^{1/2}(\xi^2-\eta^2)^{1/2}} S_{1,\ell}(\eta) R^{(3)}_{1,\ell}(\xi) \right.$$

$$\left. \left. + \frac{(\xi^2-1)^{1/2}}{(\xi^2-\eta^2)^{1/2}} S_{1,\ell}(\eta) \frac{dR^{(3)}_{1,\ell}(\xi)}{d\xi} \right] \hat{n} \right\} \tag{36}$$

We will concentrate on an idealized case of antennas with lengths that are multiple half-wavelengths. In this special case,

$$k\frac{D}{2} = P\frac{\pi}{2}\ , \text{ or } D = P\frac{\lambda}{2}$$

where P is an integer. The equations now simplify immensely. Before writing them, we must discuss the implications of symmetrical excitation. Due to this symmetry the angular functions must be symmetric; this implies ℓ must be odd [15]. In addition, P must be odd so that the angular functions are finite at $\eta = \pm 1$. The resulting simplifications follow.

$$R^{(3)}_{1,2\ell-1}(\xi) = \frac{\exp\left[+ i\frac{\pi}{2}(P\xi-2\ell)\right]}{P\frac{\pi}{2}(\xi^2-1)^{1/2}} = \frac{(-1)^{\ell}\, e^{+ i P\frac{\pi}{2}\xi}}{P\frac{\pi}{2}(\xi^2-1)^{1/2}} \tag{37}$$

where we let $\ell = 2\ell-1$ since it must be odd.

$$S_{1,2\ell-1}(\eta) = \frac{(-1)^{\ell-1}(2\ell)!}{2^{2\ell-1}(\ell-1)!\ell!}\ \frac{\cos P\frac{\pi}{2}\eta}{(1-\eta^2)^{1/2}} \equiv f(\ell)\ \frac{\cos P\frac{\pi}{2}\eta}{(1-\eta^2)^{1/2}} \tag{38}$$

Also,

$$\frac{dR}{d\xi} = R\left[+ i P\frac{\pi}{2} - \frac{\xi}{(\xi^2-1)}\right]$$

$$\frac{dS}{d\eta} = f(\ell)\left[- P\frac{\pi}{2}\frac{\sin(P\frac{\pi}{2}\eta)}{(1-\eta^2)^{1/2}} + \frac{\eta\cos(P\frac{\pi}{2}\eta)}{(1-\eta^2)^{3/2}}\right] \tag{39}$$

Now, we rewrite the fields substituting the above simplifications.

$$c\bar{B} = \left[\sum_{\ell=1}^{\infty} a_{2\ell-1} f(\ell)(-1)^{\ell}\right] \frac{\cos(P\frac{\pi}{2}\eta)}{(1-\eta^2)^{1/2}} \frac{e^{+i\,P\frac{\pi}{2}\xi\,-i\omega t}}{P\frac{\pi}{2}(\xi^2-1)^{1/2}}\,\hat{\phi} \qquad (40)$$

If we let $K \equiv \left[\sum_{\ell=1}^{\infty} a_{2\ell-1} f(\ell)(-1)^{\ell}\right]$, then

$$\bar{E} = K \frac{e^{+i\,P\frac{\pi}{2}\xi}\, e^{-i\omega t}}{P\frac{\pi}{2}(\xi^2-\eta^2)^{1/2}} \left[\frac{-i\,\sin(P\frac{\pi}{2}\eta)}{(\xi^2-1)^{1/2}}\,\hat{\xi} + \frac{\cos(P\frac{\pi}{2}\eta)}{(1-\eta^2)^{1/2}}\,\hat{\eta}\right] \qquad (41)$$

Note that the boundary conditions are now entirely encompassed by K, and all we assume is that the excitation provides multiple half-wavelengths.

It is also useful to write the fields along the spherical coordinate directions, as our measurements will be made while approaching or receding along the radial direction. The magnetic field does not change; the electric field is:

$$\bar{E} = K \frac{e^{+i\,P\frac{\pi}{2}\xi}\, e^{-i\omega t}}{P\frac{\pi}{2}(\xi^2-\eta^2)(\xi^2+\eta^2-1)^{1/2}} \left\{\left[-i\xi\sin(P\tfrac{\pi}{2}\eta) + \eta\cos(P\tfrac{\pi}{2}\eta)\right]\hat{r}\right.$$

$$\left. + \left[-\frac{i\eta(1-\eta^2)^{1/2}\sin(P\frac{\pi}{2}\eta)}{(\xi^2-1)^{1/2}} - \frac{\xi(\xi^2-1)^{1/2}\cos(P\frac{\pi}{2}\eta)}{(1-\eta^2)^{1/2}}\right]\hat{\theta}\right\} \qquad (42)$$

We must next determine the frequency shift function "η" (not to be confused with the coordinate η). For the prolate case, the values of "η" can be determined exactly.

First, the magnetic field is relatively simple. Measurement must be made along the ϕ direction to some extent, or no field is present; for now, we will assume $\hat{n} = \hat{\phi}$. Then, if we notice the phase,

$$\theta = P \frac{\pi}{2} \xi - \omega t = k \frac{D}{2} \xi - \omega t, \tag{43}$$

and we use

$$\eta = \frac{\hat{\beta} \cdot \nabla}{k} (\theta)$$

we obtain

$$"\eta_B" = s \left[\frac{\xi(\xi^2-1)}{(\xi^2-\eta^2)(\xi^2+\eta^2-1)^{1/2}}\right] \tag{44}$$

$$\simeq s \left(1 - \frac{1}{2} \sin^2\theta \frac{\left(\frac{D}{2}\right)^2}{r^2}\right) \tag{45}$$

where we have used the expansions

$$\xi \simeq \left(\frac{r}{D/2}\right) \left(1 + \frac{1}{2} \sin^2\theta \frac{(D/2)^2}{r^2}\right), \text{ and}$$

$$\eta \simeq \cos\theta \quad . \tag{46}$$

Then, in the equatorial plane,

$$"\eta_B" \simeq s \left(1 - \frac{1}{8} \frac{D^2}{r^2}\right) . \tag{47}$$

This is exactly the same result that came out of the general current source discussions of Chapter 1 and Appendix I.

The electric field is much more complicated. The result for $\overline{E} \cdot \hat{\theta}$ is

$$"\eta_E"_\theta = s \left\{ \frac{\xi\,(\xi^2-1)}{(\xi^2-\eta^2)(\xi^2+\eta^2-1)^{1/2}} + \right.$$

$$\left. \frac{\eta(1-\eta^2)}{P\,\frac{\pi}{2}} \frac{[-\,(\xi^2-1)\xi(3\xi^2+3\eta^2-2)\,\frac{\sin P\pi\eta}{2} + \eta(1-\eta^2)\,\frac{P\pi}{2}\,\xi\,(\xi^2-1)]}{(\xi^2-\eta^2)(\xi^2+\eta^2-1)^{1/2}[\eta^2(1-\eta^2)^2\sin^2(\frac{P\pi}{2}\,\eta) + \xi^2(\xi^2-1)^2\cos^2(P\,\frac{\pi}{2}\,\eta)]} \right\},$$

(48)

and for $\overline{E} \cdot \hat{r}$ is

$$"\eta"E_r = s \left\{ \frac{\xi\,(\xi^2-1)}{(\xi^2-\eta^2)(\xi^2+\eta^2-1)^{1/2}} - \right.$$

$$\left. \frac{\xi\,\eta\,[(\xi^2+\eta^2-2)\,\frac{\sin\,p\pi\eta}{2} + \frac{p\pi}{2}\,\eta\,(1-\eta^2)]}{\frac{p\pi}{2}\,(\xi^2-\eta^2)(\xi^2+\eta^2-1)^{1/2}[\eta^2\cos^2(\frac{p\pi}{2}\,\eta)+\xi^2\sin^2(\frac{p\pi}{2}\,\eta)]} \right\}.$$

(49)

In the equatorial plane, the coordinate $\eta = 0$ and the second terms vanish for both θ and r so that the identical result applies;

$$"\eta_E" \simeq s\,(1 - \frac{1}{8}\,\frac{D^2}{r^2})\,. \qquad (50)$$

Several results should be noted for these fields. First, fields along directions other than $\hat{\theta}$ for $\overline{E}$, and ϕ for $\overline{B}$, vanish in the Fresnel zone, i.e. there are no other "radiating" components, and thus no Fresnel

zone Doppler effects. The radial component of $\bar{E}$ has relatively small amplitude and may not be detectable where these approximations are valid. Also, the electrically large criterion did not play a role in the "first order" results presented; i.e. η_B and η_E are independent of P to this order. However, for measurement the possibility that P may be large is important and will be used in Chapter 3. The frequency measured in the cases above is the same for all components.

$$\omega' = \omega\,(1 - \beta\eta)$$

$$\simeq \omega\ \left[1 - \beta s\ (1 - \frac{D^2}{8r^2})\right] , \tag{51}$$

thus no information is available on the source except the distance to the observer. From the above equation (51), it may be seen that the phase velocity

$$v_{ph} = \frac{c}{1 - \frac{D^2}{8r^2}} \quad , \qquad \lambda' = \frac{\lambda}{1 - \frac{D^2}{8r^2}} \tag{52}$$

i.e. the phase velocity and wavelength increase in the near-zone as shown. Finally the equivalent dielectric is

$$\varepsilon(r) \simeq \varepsilon_0(1 - \frac{D^2}{4r^2}) , \tag{53}$$

so that dielectric variations of the same order of magnitude would lead to mistaken results.

Since η can be calculated exactly for the prolate spheroid, it is interesting to record and discuss the results in comparison with the infinitesimal dipole case. η_B, η_{E_θ}, and η_{E_r} are plotted for various angles of approach (i.e. θ not just equal $\pi/2$) and for various P values. The earliest changes from far field values occur as expected (as $\frac{D^2}{8r^2}$), see Figures 4-11.

Figures 4 and 5 depict η for an electrically large antenna ($\frac{D}{\lambda} > 10$). The results show that the shifts predicted occur to $\frac{R}{D} < 2$, where $\frac{D^2}{8r^2}$ is in error by less than 5%. As $\frac{R}{D} < 2$ the frequency shifts approach zero, as we might expect — a smooth transition from blue to red as the source passes the observer

$$\omega' = \omega\,(1 - \beta) \rightarrow \omega \rightarrow \omega\,(1 + \beta)\ .$$

For larger antennas similar results are obtained (data were taken to $\frac{D}{\lambda} \simeq 1000$). Several angles were used for approach of the source; all yielded the identical results.

The smaller antennas, however, show the effects presented for the infinitesimal dipole. The magnetic field has no inverse effect, however the electric field does. This is shown in Figures 6 through 11. The first near zone shifts in η are as predicted to $\frac{R}{D} \sim 2$. (Recall the shift was independent of p or $\frac{D}{\lambda}$ to this order). Below $\frac{R}{D} \sim 2$, the inverse effects may occur. For the case presented, with $\frac{D}{\lambda} = 0.5$, $\frac{R}{D} < 2$ implies $\frac{R}{\lambda} < 1$; we thus note that inverse effects are only observed in the reactive near field within a wavelength or so of the source.

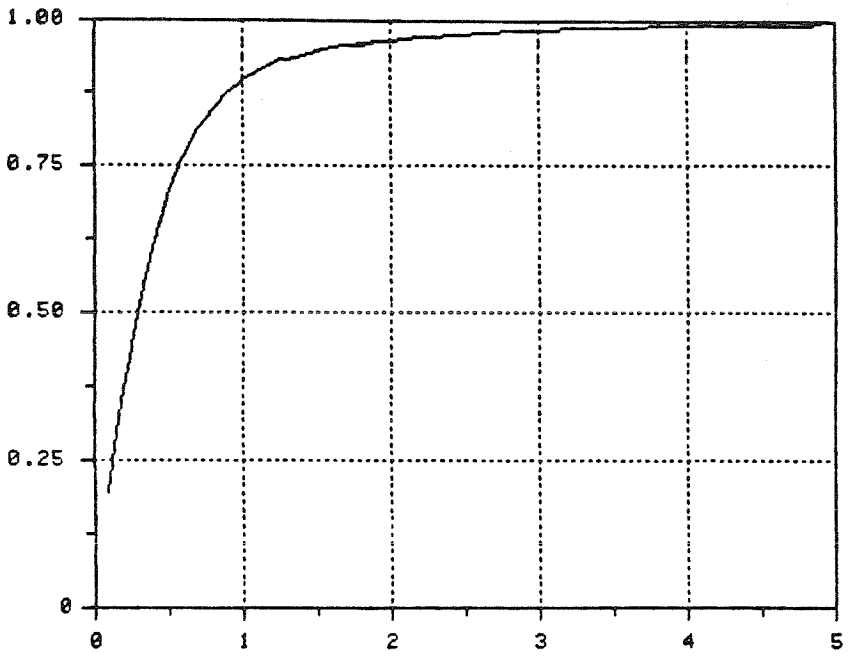

Figure 4

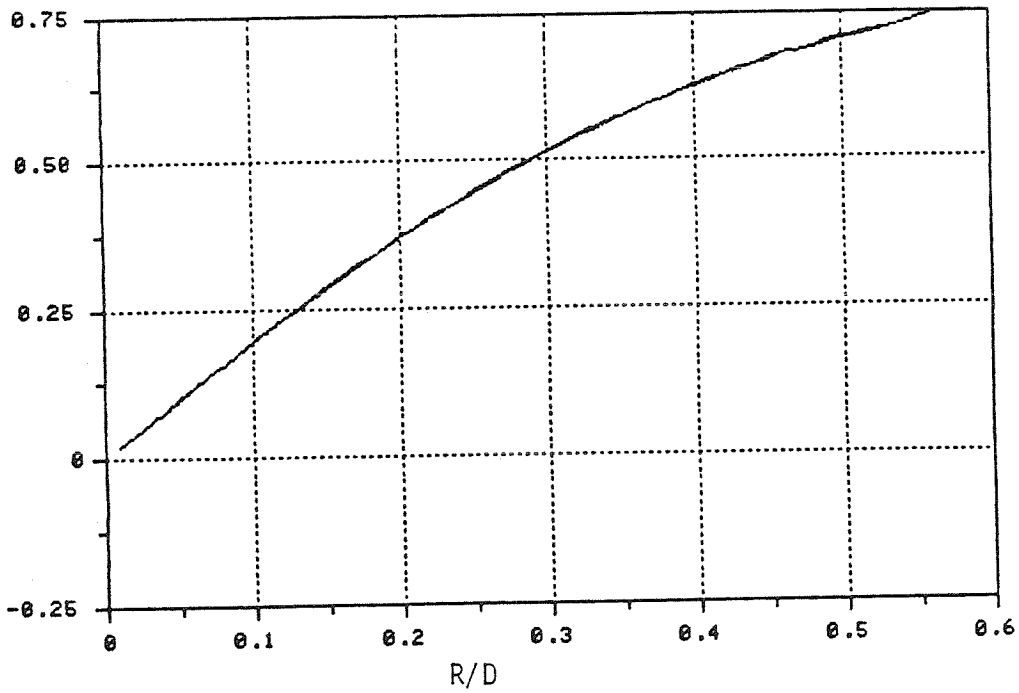

Figure 5

Prolate Spheroidal Antenna $(\frac{D}{\lambda} = 10.5,\ p = 21)$

η is same for all fields $(\overline{E},\ \overline{B})$

Figure 6

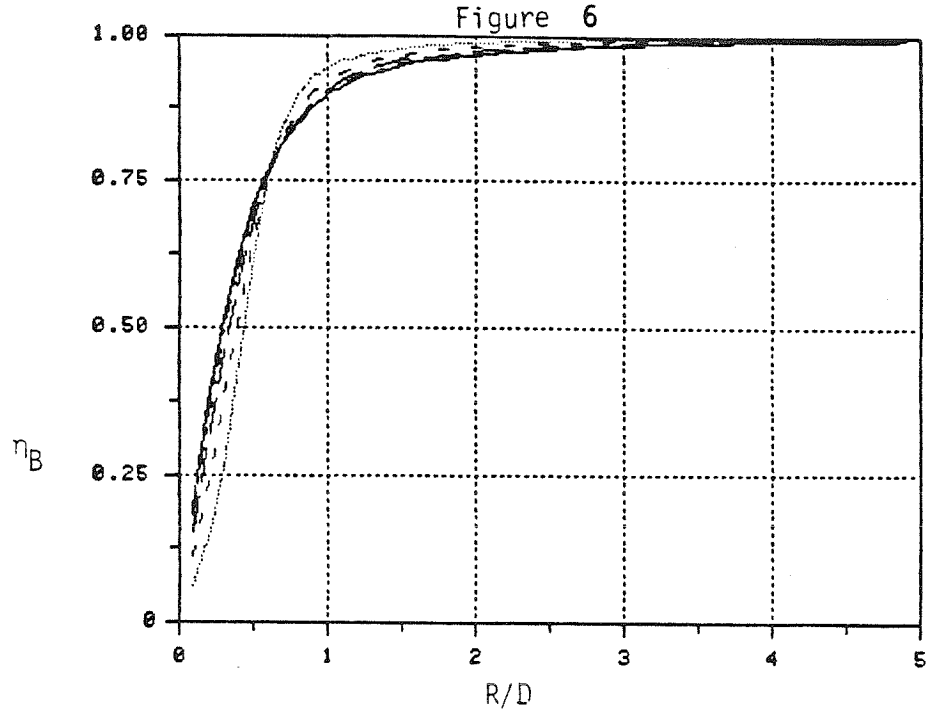

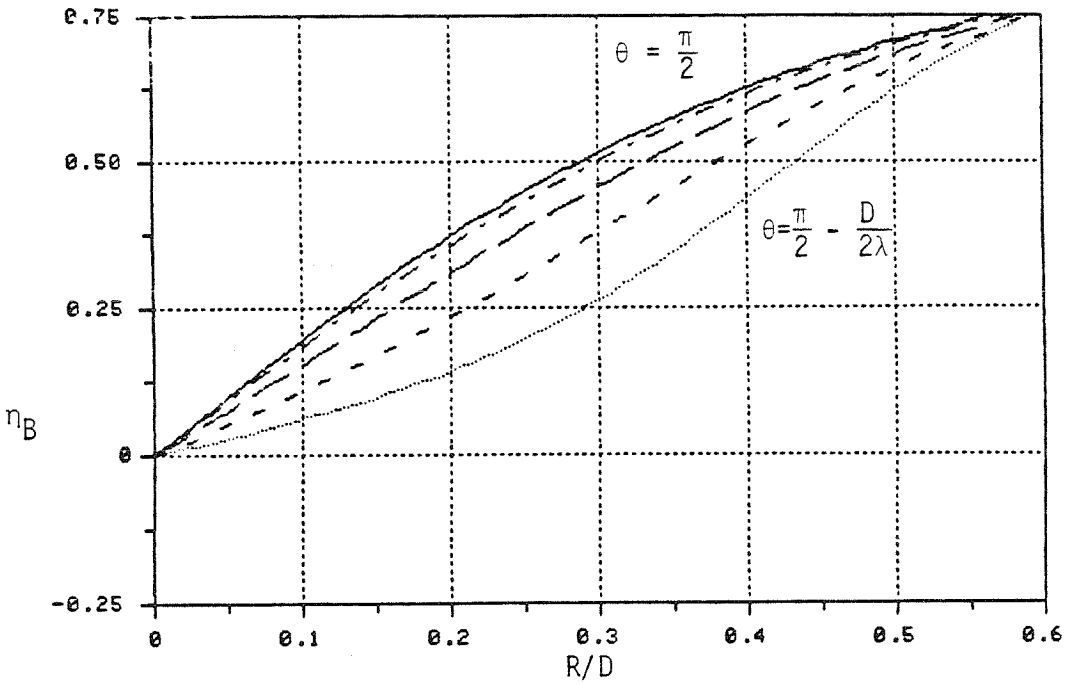

Figure 7

Prolate Spheroidal Antenna ($\frac{D}{\lambda} = 0.5$, $p = 1$)

Curves shown correspond to successively larger angles off axis,

i.e. $\theta - \frac{\pi}{2} = 0, \frac{-1}{8}\frac{D}{\lambda}, \frac{-1}{4}\frac{D}{\lambda}, \frac{-3}{8}\frac{D}{\lambda}, \frac{-1}{2}\frac{D}{\lambda}$

Figure 8

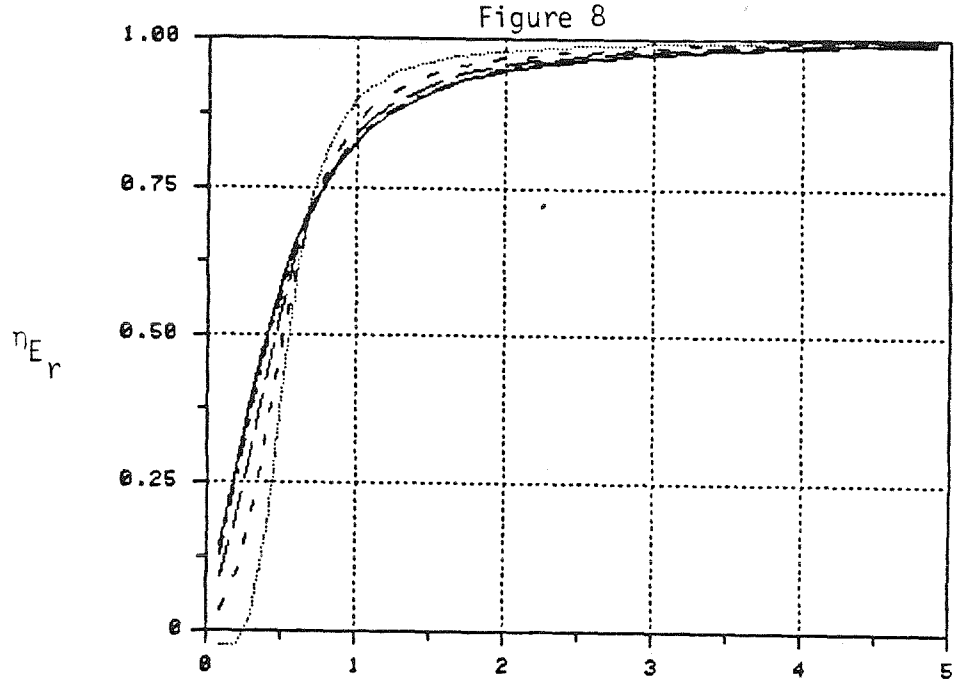

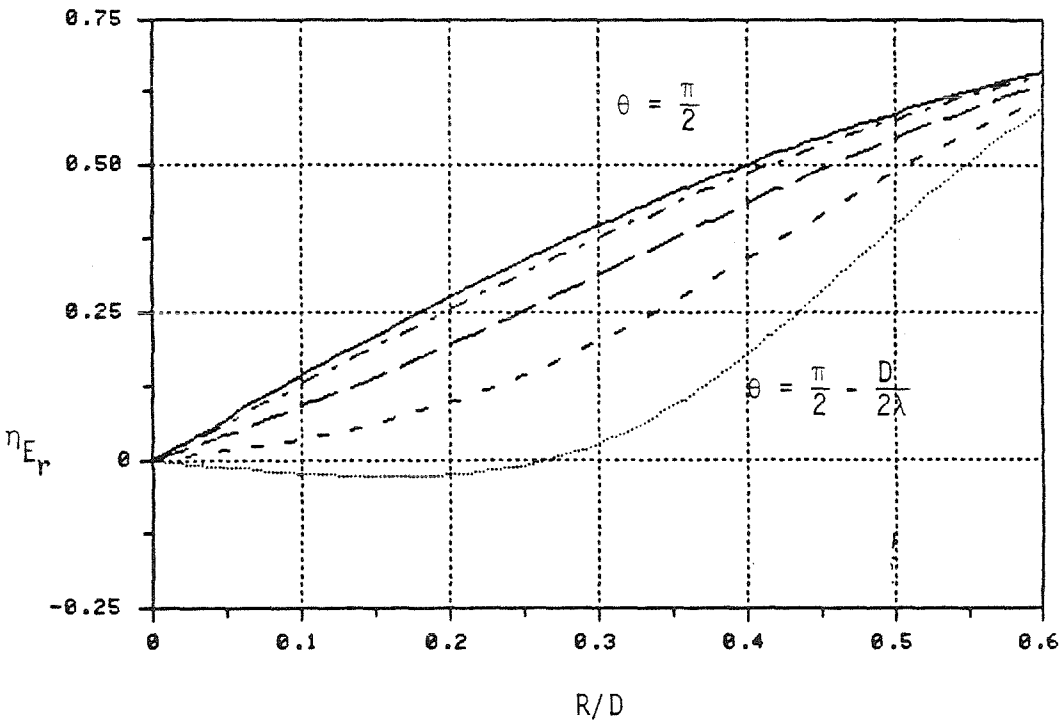

Figure 9

Prolate Spheroidal Antenna ($\frac{D}{\lambda} = 0.5$, $p = 1$)

Curves correspond to same angles off axis as in Figures 6, 7.

Note "inverse" Doppler effects for $\eta < 0$.

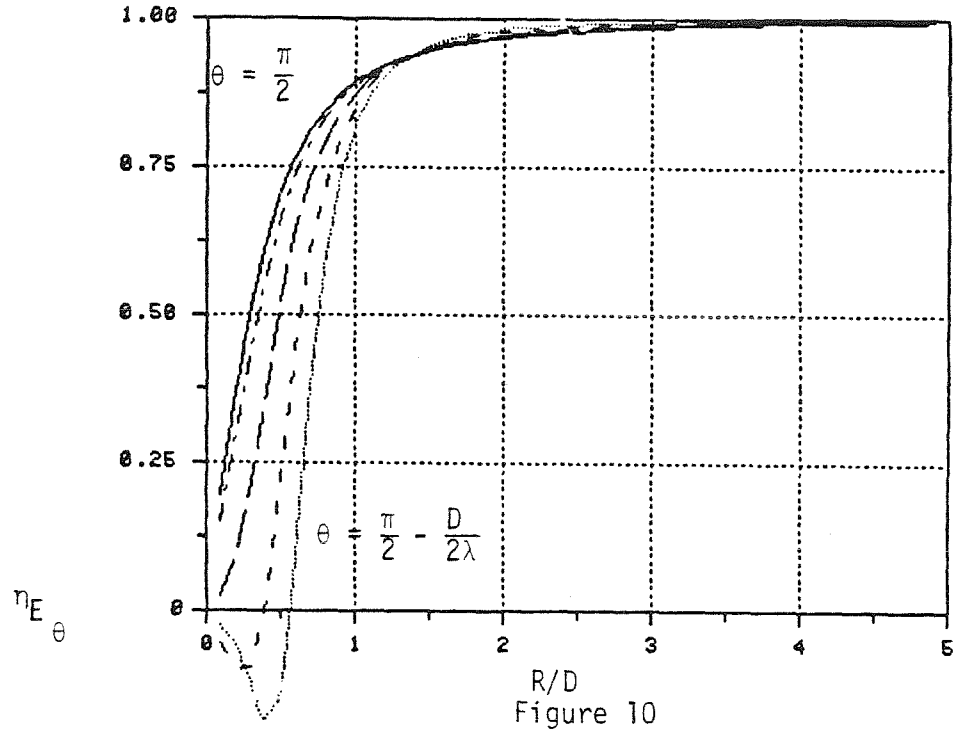

Figure 10

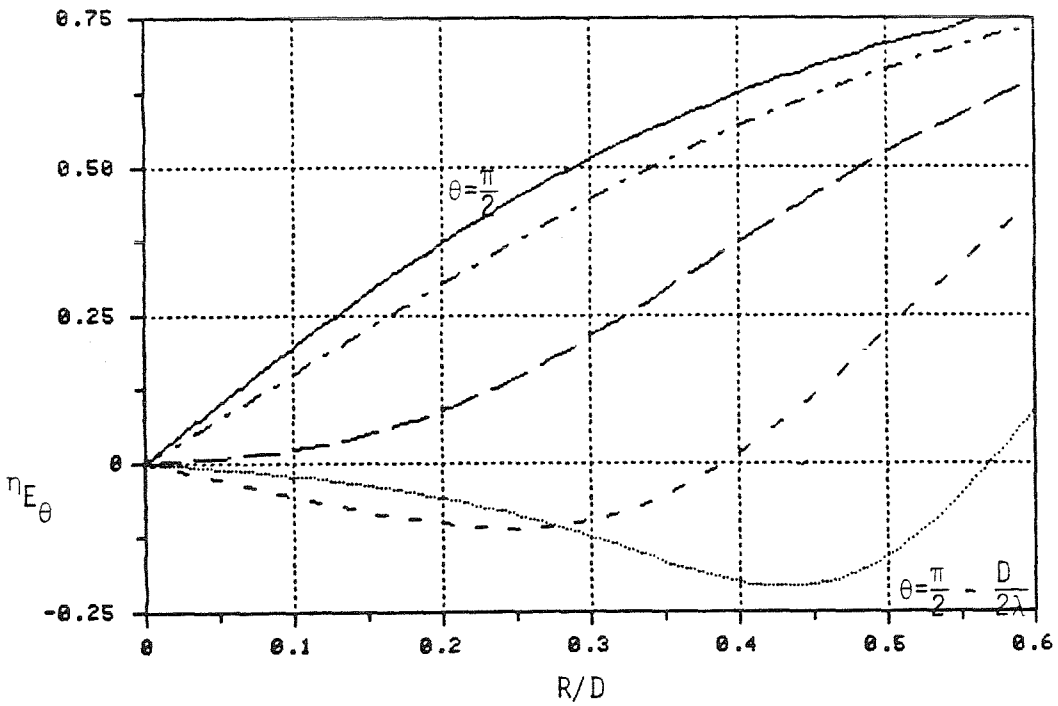

Figure 11

Prolate Spheroidal Antenna ($\frac{D}{\lambda}$ = 0.5, p = 1)

Same angles as in Figures 6, 7. Again, note inverse effects.

C. Circular Aperture Antenna

As a second example, we will investigate the circular aperture. We will assume Fresnel approximations where the total aperture field is approximated by the incident aperture field, and observations are made only near or along the central axis of the aperture (see Appendix II).

We will assume the incident field is a uniform plane wave propagating in the y direction;

$$\bar{E}_i = K\, e^{i(ky-\omega t)}\, \hat{z} \quad . \tag{54}$$

Also, let the aperture be centered at the origin of the y = 0 plane, and let the circular diameter be D. We will measure the z component of the field while motion is along the y axis. The set-up then looks very similar to that shown in Figure II-1 of Appendix II. Also referring to the Appendix, we recall equation (II-6)

$$\bar{E} \cdot \hat{n} = -i2k^2\, \frac{e^{iky}}{4\pi ky} \int_A e^{i\frac{k^2 r''^2}{2ky}}\, K\, d\bar{r}''\, e^{-i\omega t} \tag{55}$$

where we substituted the incident field for $\hat{z} \cdot \bar{E}_i$. The result for E_z is

$$\begin{aligned} E_z &= K\, e^{iky}\, (1 - e^{i\frac{k^2D^2}{8ky}})\, e^{-i\omega t} \\ &= -2iK \sin\left(\frac{k^2D^2}{16ky}\right) e^{iky}\, e^{i\frac{k^2D^2}{16ky}}\, e^{-i\omega t} \end{aligned} \tag{56}$$

In this equation it may be seen that there are two fundamentally separate waves propagating in the Fresnel zone, a plane wave and a scattered wave. These two waves interfere as may be seen in second equation, until in the far field one wave remains.

This case presents problems for frequency measurement since there are actually two frequencies present. The definition of η assumes a monochromatic signal with slowly varying frequency, and an even more slowly varying amplitude. With the present definition, η becomes

$$\eta = s\left(1 - \frac{D^2}{16y^2}\right)$$

Here s indicates $\begin{cases} +1 \text{ when receding from aperture} \\ -1 \text{ when approaching aperture} \end{cases}$

This is just the derivative of the phase. The amplitude, however, varies as rapidly as the near-zone correction term. This eliminates the possibility of measuring the frequency shift as defined.

The amplitude fluctuations are a common feature of aperture sources. They are caused by the interference of the incident wave and scattered wave in the Fresnel region. The circular aperture is a particularly appropriate example. If the aperture is divided into annular rings, sometimes called "Fresnel Zones" [8], with the path length from successive rings to a point along the axis of R, $R + \frac{\lambda}{2}$, $R + \lambda$, $R + 3\frac{\lambda}{2}$, ... it can be observed that successive rings interfere; they are out of phase by 180^0. Depending upon the aperture diameter some finite number of the rings will fit. If an even number of rings

are present the field is nearly zero. If an odd number is included the field takes on its maximum locally.

This simple idea predicts exactly the same results as those obtained mathematically for the circular aperture and gives some insight into possible general problems with amplitude variations in the Fresnel region. It should be noted, however, that if the aperture distribution does not have uniform phase, as with plane wave incidence, the interference pattern will change. The prolate spheroid has a current distribution which is not uniform. In the limit of a very thin spheroid the current goes as cos(kz).

D. Observations

Before we discuss the measurability of the frequency shift, we should observe some of the implications of the results for the examples just given.

The general formulae of Chapter 1 and these examples demonstrate tne generality of near-zone Doppler effects. Several more specific examples could be given, however, the point has been made that the effects do exist as originally suggested [4] and not just for the inifinitesimal dipole, but for most sources. We then further suggest that the results of this chapter have broader application.

The prolate spheroidal fields (40) and (41), reduce in the far zone to those of simple center driven wire antennas [7].

$$c\overline{B} \sim K \frac{e^{i(kr-\omega t)}}{kr} \quad \frac{\cos(k \frac{D}{2} \cos\theta)}{\sin\theta} \hat{\phi}$$

$$\overline{E} \sim K \frac{e^{i(kr-\omega t)}}{kr} \quad \frac{\cos(k \frac{D}{2} \cos\theta)}{\sin\theta} \hat{\theta}$$

where $k \frac{D}{2} = p \frac{\pi}{2}$.

The same frequency shift predicted might then be expected to occur for thin wire antennas with similar excitation. Thus, the first near-zone effects might be

$$\omega' \simeq \omega \left(1 - \beta s\left(1 - \frac{D^2}{8r^2}\right)\right)$$

where D is the wire length, and $r \simeq vt$.

The circular aperture with a plane wave incident is certainly not an isolated case of the applicability of the aperture results of Chapter 1 and Appendix II. Other shaped apertures, like elliptical or square should have similar Fresnel zone shifts; and other incident fields, should produce some shifts, although they will not be identical to those of the plane wave. However, there probably will be similar complications with interfering waves for other apertures that may preclude measurable effects; each case would have to be dealt with individually.

There seems little doubt, however, that the frequency shifts of the near-zone fields generally exist. Now we just have to measure them.

CHAPTER 3 - MEASURABILITY AND PRACTICAL APPLICATION OF RESULTS

The questions of measurability fall into three categories:

(1) frequency definition,

(2) near-zone measurement problems, and

(3) spatial extent and magnitude of effects.

The definition of frequency as the time derivative of the received phase is applicable so long as the amplitude of the field varies slowly compared with the phase. As was pointed out in the circular aperture example of the last chapter, care must be taken in the Fresnel zone to assure that amplitude variations occurring during the measurement interval do not interfere with the frequency determination. For the prolate case in the equatorial plane it can be seen that the variations are slow.

$$E_\theta \simeq \frac{K}{k\frac{D}{2}\xi} e^{i(k\frac{D}{2}\xi - \omega t)} = K\frac{e^{i(\theta - \omega t)}}{k\frac{D}{2}(1 + r^2/(D/2)^2)^{1/2}}$$

So,

$$A \sim \frac{1}{kr}\left(1 - \frac{D^2}{8r^2}\right) .$$

Thus for large kr, the amplitude variations may be held small so long as $\frac{D}{\lambda} >> 1$. The main component of variation is the normal $\frac{1}{kr}$ dependence of spherical waves. For the circular aperture case, the amplitude variations are not small, however, and our frequency definition is no longer precise. The interfering waves provide a common problem in FM receivers [16]. In this case it is especially severe since the

amplitudes of the two waves are equal.

Other near-zone measurement problems result from the interference of the measuring device with the near-zone field. This is basically a question of relative size and location. The transmitting antenna must be large compared with the receiver aperture and device size, so that no appreciable change is made to the near-zone fields of the source. Also, the receiver should be located as far from the source as possible during measurement to further reduce the possibility of interference. The many issues related to near-zone measurements are discussed by Dyson [6]. This article also includes an extensive bibliography on the subject.

Another "interference" problem results if the media through which the measurements are taking place has dielectric (or permeability) fluctuations that are on the same order of magnitude as the shifts. As pointed out in Chapter 1, the dielectric equivalent to the shift η is

$$\varepsilon(r) \simeq \varepsilon_0 \eta^2(r).$$

Thus, if $\varepsilon(r)$ varies as the source approaches or recedes, it may be impossible to distinguish this variation from the near-zone effects. This makes it necessary to have sufficient frequency shifts in the near-zone so that no indeterminacy will exist.

If we assume now that some devices are available to measure the fields and received frequency, then we still must be able to resolve the small shifts that are inherent with low β and in the Fresnel zone. The distance over which we can measure the frequency shift is limited;

recall $r = vt$, i.e. the source is either approaching and will pass us or receding and will soon be in the far zone.

We will now show that the required distance (time) for measuring a shift must be greater than $\lambda/|\partial\eta|$ $(\lambda/v|\partial\eta|)$, where λ is the wavelength of radiation and $|\partial\eta|$ is the near-zone shift in the η function and v is the relative velocity. To see this result, recall

$$f' = f(1 - \beta\eta) \text{ with } \omega = 2\pi f$$

where f is the transmitted frequency, β is the relative speed and η is the function of position which varies as the source approaches or recedes. The shift in frequency to be measured when $|\eta|$ changes from 1 by $\partial\eta$, i.e. $|\eta| = 1 + \partial\eta$, is:

$$|\Delta f| = f\,\beta \cdot |\partial\eta| \tag{62}$$

This requires a measurement time T, where $T \simeq \frac{1}{\Delta f} = \frac{1}{f\,\beta|\partial\eta|}$ in order to resolve the shift (from simple uncertainty arguments). The source must be near the observer long enough for this measurement to take place. If R is the available measurement distance, or

$$R = \beta c t, \tag{63}$$

then in order to measure (resolve) the shift,

$$R > \beta c \left(\frac{1}{f\,\beta|\partial\eta|}\right) = \frac{\lambda}{|\partial\eta|} \qquad \left(\text{or } t > \frac{\lambda}{v|\partial\eta|}\right) \tag{64}$$

i.e. $t > T$, the measurement time available must exceed the required

resolution time. Thus, in order to measure this shift it must occur a number of wavelengths from the source related to the magnitude of the shift $|\partial\eta|$. In the prolate spheroid case of Chapter 2,

$$\eta = s\left(1 - \frac{D^2}{8r_o^{\,2}}\right) \quad , \quad |\partial\eta| = \frac{D^2}{8r_o^{\,2}} \tag{65}$$

where r_o is the distance at which the shift we are going to try to resolve first occurs during approach of the source. Then,

$$R > 8\,\frac{r_o^{\,2}}{D^2}\,\lambda \tag{66}$$

for resolution; but $r_o \geq R$, and thus r_o is the maximum distance available for measurement. If r_o were available ($R = r_o$),

$$\frac{R}{8\,\frac{R^2}{D^2}\,\lambda} > 1 \quad \text{or} \quad \frac{(\frac{D}{\lambda})}{8(\frac{R}{D})} > 1 \quad . \tag{67}$$

For $\frac{R}{D} = 4$, a shift $|\partial\eta|$ of less than 1% occurs, see (65). $\frac{D}{\lambda}$ must be greater than 32 in order to resolve the shift. (Note that in this prolate case, P, the number of half-wavelengths, must be greater than 64).

An additional complication arises if the shift continues to change (i.e. η varies) during the measurement process. This variation should either be small, or, slowly increase the shift in the same direction as in the example just cited, so that some resolution is possible.

For $\frac{R}{D} = 4$ and $\frac{D}{\lambda} = 1000$ we would have 4000λ to resolve a shift $|\partial\eta|$ that begins as $\frac{1}{128}$. After a few hundred λ we would

have surely resolved the shift, and we would still be near $R \simeq 4D$.

This example dealt with approaching sources. For receding sources, as is indicated in the formula (65) the shifts are initially larger and become smaller. The resolution problem, however, is essentially the same.

The measurability of the near-zone Doppler effect has now been shown to depend on the available measurement distance, and the magnitude of the frequency shift. The general assumption that high gain or electrically large electromagnetic sources were the most useful in the near zone has been demonstrated. The choice of investigation of the Fresnel zone was thus appropriate. So, overall we have shown that for adequately large sources the near-zone Doppler effects have a real possibility of being measurable.

CHAPTER 4 - SUMMARY AND CONCLUSIONS

Summary:

The ideas of previous work with the infinitesimal dipole [4] have been extended to show the generality of near-zone Doppler effects and to indicate the possibility of measurement for electrically large antennas. Of the three interesting features brought out by the previous work;

(1) existence of near-zone effects

(2) different effects for each field component being measured, and

(3) range information availability;

all were found present to some extent for the electromagnetic sources investigated. In a zone where measurement was practical, the Fresnel zone, near-zone effects were shown to exist and range information was available to a practical limit. The resolution of range was limited to the distance through which the source moved during the measurement. The frequency shifts in the Fresnel zone for the wire antenna with low relative velocity were

$$\omega' = \omega\left(1 \pm \beta\left(1 - \frac{D^2}{8R^2}\right)\right)$$

where $\beta = \frac{v}{c}$ was the normalized relative velocity, D was the antenna length, and $R = |vt|$ was the distance between source and observer as they approached (or receded) radially. Both field components (B_ϕ, E_θ) had this same shift in the Fresnel zone and thus the information suggested by the second feature above was not available.

It was shown that in the extreme near zone of a smaller wire antenna this information was theoretically available although measurement there would be impractical.

The circular aperture example served to point out a possible pitfall in measuring frequencies in the Fresnel zone. The interfering incident and scattered waves caused amplitude fluctuations that were as large as the near-zone frequency correction, thus prohibiting the measurement, i.e. resolution, of the small additional shift.

A more general form of the Doppler shift, conducive to the understanding of the frequency shift was also described. The form was

$$\omega' = \omega \left(1 \pm \frac{v}{v_{ph}}\right)$$

where v_{ph} was the source frame phase velocity. The reasoning went as follows. The source had surfaces of constant phase which, in the near zone, were not spherical. This "distortion" of the normally spherical waves was a contributor to the Doppler shift being measured by an observer. As in the normal Doppler effect, the observer measured a different distance between the surfaces of constant phase than that identified by the source as one wavelength (2π in phase). The actual distorted waves of the near zone, however, had a slightly different distance between constant phase surfaces than those of spherical waves (or plane waves). This difference was precisely related to the frequency shift by the phase velocity as described. Thus near-zone Doppler effects were the same as far-zone Doppler effects, but

with the local phase velocity replacing the far-zone phase velocity, c. The distortion of the wave fronts produced by the proximity of the source was responsible for the correction to the normal far-zone red or blue shifts, thus producing the near-zone Doppler effects.

Conclusions:

The general theoretical existence of near zone Doppler effects has been demonstrated. These effects may be described by

$$\omega' \simeq \omega \left(1 \pm \frac{v}{v_{ph}}\right)$$

where v_{ph} is the local phase velocity and the $\pm$ signs are for approaching and receding. The measurable effects found for the sources investigated were in the Fresnel zone. The previous indications of the dipole work that range information was available were shown to be generally true. The indication that additional information might be available by measuring each field component separately was shown not to be useful in the Fresnel zone. Small corrections to the far-zone Doppler shifts were found to be measurable but no measurable "inverse" Doppler effects were discovered.

APPENDIX I - CURRENT SOURCE FIELDS

The current source fields will be derived from Maxwell's equations exactly. Then, a series expansion of the amplitude in terms of $(kr)^{-1}$ will be used to determine the approximate fields and the associated Doppler effects as the source approaches the observer. As in Chapter 1, we will assume that terms only of first order in β, the normalized relative velocity, need to be kept.

The fields due to a harmonic current distribution are written as [7]. (See Figure I-1):

$$\bar{E} = i\omega k\mu \int \left[\bar{\bar{u}} + \frac{1}{k^2} \nabla \nabla\right] \frac{e^{ikR}}{4\pi kR} \cdot \bar{J}(\bar{r}')d\bar{r}' \, e^{-i\omega t} \tag{I-1}$$

$$c\bar{B} = \omega k\mu \int \left(\frac{1}{k} \nabla\right) \frac{e^{ikR}}{4\pi kR} \times \bar{J}(\bar{r}')d\bar{r}' \, e^{-i\omega t} \tag{I-2}$$

where $R = |\bar{r} - \bar{r}''|$, $\bar{r}$ being the vector from the origin of the source frame to the point where the field is measured and $\bar{r}''$ being a vector from the source origin to a point of the current distribution, ∇ applies only to the point of measurement $(\bar{r})$; and $\bar{\bar{u}}$ is the unit dyadic. After the derivatives are taken, the fields become:

$$\bar{E} = i\omega\mu k \int \frac{e^{ikR}}{4\pi kR} \left\{ \bar{\bar{u}}\left[\frac{k^2R^2+ikR-1}{k^2R^2}\right] + \hat{R}\hat{R}\left[\frac{-k^2R^2-3ikR+3}{k^2R^2}\right] \right\} \cdot \bar{J}(\bar{r}'')d\bar{r}'' \, e^{-i\omega t} \tag{I-3}$$

$$c\bar{B} = \omega\mu k \int \frac{e^{ikR}}{4\pi kR} \left[\frac{ikR-1}{kR}\right] \hat{R} \times \bar{J}(\bar{r}'')d\bar{r}'' \, e^{-i\omega t} \tag{I-4}$$

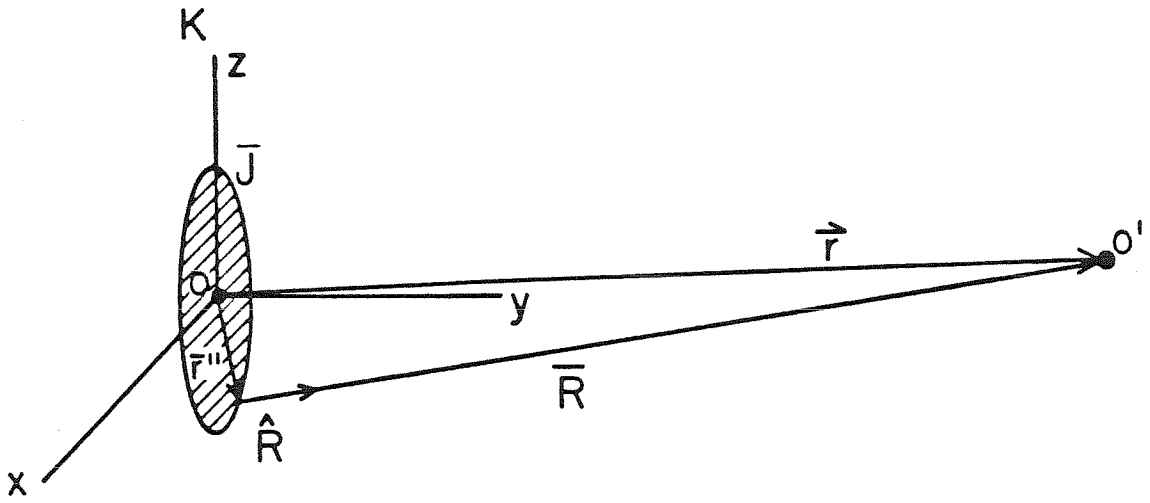

Figure I-1 Current Source Coordinates

O is the origin of the source frame K

O' is the origin of the observer frame K'

$\bar{J}$ is the vector current density

where $\hat{R} = \dfrac{\bar{r} - \bar{r}''}{|\bar{r} - \bar{r}''|}$.

These are the exact field equations. We will also need the derivatives of these equations since

$$\eta = \text{Imag}\left\{ \frac{\hat{\beta} \cdot \frac{\nabla}{k} (\bar{E} \cdot \hat{n})}{\bar{E} \cdot \hat{n}} \right\}.$$

The required derivatives may be obtained from the following exact expressions where vector component subscripts are used to retain the proper order.

$$\frac{\nabla}{k} \bar{E} \equiv \frac{1}{k} \partial_\ell E_m = is\hat{\beta}_\ell E_m +$$

$$i\omega\mu k \int \frac{e^{ikR}}{4\pi kR} \left\{ i(\hat{R}_\ell - \hat{\beta}_\ell s)[u_{mn}(\frac{k^2R^2+ikR-1}{k^2R^2}) + \hat{R}_m\hat{R}_n(\frac{-k^2R^2-3ikR+3}{k^2R^2})] \right.$$

$$+ \hat{R}_\ell[u_{mn}(\frac{-k^2R^2-2ikR+3}{k^3R^3})] + \hat{R}_\ell[\hat{R}_m\hat{R}_n(\frac{3k^2R^2+12ikR-15}{k^3R^3})]$$

$$\left. + u_{\ell n}\hat{R}_m\ (\frac{-k^2R^2-3ikR+3}{k^3R^3}) \right\} J_n d\bar{r}''\ e^{-i\omega t} \qquad \text{(I-5)}$$

$$\frac{\nabla}{k} c\bar{B} = \frac{1}{k} \partial_\ell cB_m = is\hat{\beta}_\ell cB_m +$$

$$\omega\mu k \int \frac{e^{ikR}}{4\pi kR} \left\{ i(\hat{R}_\ell - \hat{\beta}_\ell s)[\frac{ikR-1}{kR}]\ (\hat{R} \times \bar{J})_m + \hat{R}_\ell[\frac{-2ikR+3}{k^2R^2}]\ (\hat{R} \times \bar{J})_m \right.$$

$$\left. + [\frac{ikR-1}{k^2R^2}]\ (\bar{\bar{u}} \times J)_{\ell m} \right\} d\bar{r}''\ e^{-i\omega t} \qquad \text{(I-6)}$$

The "$\hat{\beta}s$" term has been pulled out to simplify results. Recall, $s = \begin{cases} +1 & t > 0 \\ -1 & t < 0 \end{cases}$ and in order to calculate η we need

$$\hat{\beta} \cdot \frac{\nabla}{k} (\bar{E} \cdot \hat{n}) \text{ or } \hat{\beta} \cdot \frac{\nabla}{k} (c\bar{B} \cdot \hat{n})$$

where $\hat{n}$ is the unit vector along the field component being measured. If the measurement point is taken at the origin of the observer frame, then $\hat{\beta}s = \hat{r}$ as shown in Figure 1 of Chapter 1. $\hat{R}$ reduces in first order to $\hat{r}$ so that the first term in both integrals vanishes to first order. The purpose in writing these functions out explicitly is for series expansions beyond the normal Fresnel zone case. First, we will use the Fresnel case; expansions beyond the first order in amplitude will then be used only to show the limitations of the approximations used.

The approximations to be made are:

(1) $\hat{r} \cdot \hat{r}'' = 0$, the antenna will approach us oriented orthogonal to the motion, and with minimal radial extent

(2) $\hat{n} \cdot \hat{r} = 0$, we will measure the fields along directions orthogonal to the motion; also no Fresnel field exists in the radial direction

(3) $\hat{r} \cdot \bar{J}$, assume essentially no radial current

(4) $e^{ikR} \simeq e^{ikr} e^{i\frac{k^2 r''^2}{2kr}}$, we will expand the phase to second order

The field functions then become:

$$\bar{E} \cdot \hat{n} = i\omega\mu k \frac{e^{ikr}}{4\pi kr} \int e^{i\frac{k^2 r''^2}{2kr}} (\hat{n} \cdot \bar{J})\, d\bar{r}''\, e^{-i\omega t} \qquad \text{(I-7)}$$

$$c\bar{B} \cdot \hat{n} = i\omega\mu k \frac{e^{ikr}}{4\pi kr} \int e^{i\frac{k^2 r''^2}{2kr}} (\hat{n} \cdot (\hat{r} \times \bar{J}))\, d\bar{r}''\, e^{-i\omega t} \qquad \text{(I-8)}$$

$$\hat{\beta} \cdot \frac{\nabla}{k} (\bar{E} \cdot \hat{n}) =$$

$$is(\bar{E} \cdot \hat{n}) + i\omega\mu ks \int \left[-\frac{1}{kr} - \frac{ik^2 r''^2}{2k^2 r^2}\right] e^{i\frac{k^2 r''^2}{2kr}} (\hat{n}\cdot\bar{J}) d\bar{r}''\, e^{-i\omega t} \qquad \text{(I-9)}$$

$$\hat{\beta} \cdot \frac{\nabla}{k} (c\bar{B} \cdot \hat{n}) =$$

$$is(c\bar{B}\cdot\hat{n}) + i\omega\mu ks \frac{e^{ikr}}{4\pi kr} \int \left[-\frac{1}{kr} - \frac{ik^2 r''^2}{2k^2 r^2}\right] e^{i\frac{k^2 r''^2}{2kr}} (\hat{n}\cdot(\hat{r}\times\bar{J})) d\bar{r}''\, e^{-i\omega t} \qquad \text{(I-10)}$$

Now η may be written

$$\eta_E = \text{Imag} \left\{ \frac{\hat{\beta} \cdot \frac{\nabla}{k} (\bar{E} \cdot \hat{n})}{(\bar{E} \cdot \hat{n})} \right\} \text{, or}$$

$$\eta_E = s \left(1 - \frac{1}{k^2 r^2} \text{Real} \left\{ \frac{\int \frac{1}{2} k^2 r'^2 e^{i\frac{k^2 r''^2}{2kr}} (\hat{n}\cdot\bar{J}) d\bar{r}''}{\int e^{i\frac{k^2 r''^2}{2kr}} (\hat{n}\cdot\bar{J}) d\bar{r}''} \right\} + \ldots \right) \qquad \text{(I-11)}$$

Also, for the magnetic field

$$\eta_B = \text{Imag}\left\{\frac{\hat{\beta}\cdot\frac{\nabla}{k}(c\bar{B}\cdot\hat{n})}{(c\bar{B}\cdot\hat{n})}\right\}, \text{ or}$$

$$\eta_B = s\left(1 - \frac{1}{k^2r^2}\,\text{Real}\left\{\frac{\int\frac{1}{2}\,k^2r''^2\,e^{i\frac{k^2r''^2}{2kr}}\,(\hat{n}\cdot(\hat{r}\times\bar{J}))d\bar{r}''}{\int e^{i\frac{k^2r''^2}{2kr}}\,(\hat{n}\cdot(\hat{r}\times\bar{J}))d\bar{r}''}\right\} + \ldots\right) \qquad \text{(I-12)}$$

The frequency observed is then $\omega' \simeq \omega\,(1 - \beta\eta)$.

As shown in Chapter 1, the first term after the far field term in the expansion for η is second order in $(kr)^{-1}$. The expressions in parentheses will commonly be on the order of $\frac{1}{8}k^2D^2$, where D is the largest dimension of the source. Thus,

$$\eta \simeq 1 - \frac{1}{8}\frac{D^2}{r^2} + \ldots \qquad \text{(I-13)}$$

For $r \sim 4D$, the correction in the Fresnel field is less than 1%.

It should be noted that the ratio given in parentheses is only part of a series expansion. The following expansions show the limits of the approximation and point out that if the numerator integral were significant in comparison with $(kr)^2$, a similar term would appear in the extended expansion of the field itself (in the denominator). If terms in both the numerator and denominator are expanded to second order —

$$\eta_E = s\left(1+\text{Imag}\left\{\frac{\int e^{i\frac{k^2r''^2}{2kr}}\left[-\frac{1}{kr}-\frac{i}{k^2r^2}\left(2+\frac{1}{2}k^2r''^2\right)\right](\hat{n}\cdot\bar{J})d\bar{r}''}{\int e^{i\frac{k^2r''^2}{2kr}}\left\{\left[1+\frac{i}{kr}-\frac{\left(1+\frac{1}{2}k^2r''^2\right)}{k^2r^2}\right]\hat{n}\cdot\bar{J}-\frac{k^2r''^2}{k^2r^2}(\hat{n}\cdot\hat{r}'')(\hat{r}''\cdot\bar{J})\right\}d\bar{r}''}\right\}\right) \tag{I-14}$$

$$\eta_B = s\left(1+\text{Imag}\left\{\frac{\int e^{i\frac{k^2r''^2}{2kr}}\left[-\frac{1}{kr}-\frac{i}{k^2r^2}\left(2+\frac{1}{2}k^2r''^2\right)\right](\hat{n}\cdot(\hat{r}\times\bar{J}))d\bar{r}''}{\int e^{i\frac{k^2r''^2}{2kr}}\left[1+\frac{i}{kr}-\frac{k^2r''^2}{k^2r^2}\right](\hat{n}\cdot(\hat{r}\times\bar{J}))d\bar{r}''}\right\}\right) \tag{I-15}$$

We see that the quadratic amplitude term ($k^2r''^2$) also appears in the denominator, thus the near-zone corrections to η in (I-11) and (I-12) cannot be large or the approximations used break down. Thus, η cannot change sign in the Fresnel region, i.e. no inverse Doppler effects can occur there.

APPENDIX II - APERTURE DISTRIBUTIONS

The fields to the right of the aperture are given by [17] integrals over the aperture (A) fields:

$$\bar{E} = 2k^2 \frac{\nabla}{k} \times \int_A (\hat{a} \times \bar{E}'') \frac{e^{ikR}}{4\pi kR} \, d\bar{r}'' \,, \tag{II-1}$$

and

$$c\bar{B} = 2k^2 \frac{\nabla}{k} \times \int_A (\hat{a} \times c\bar{B}'') \frac{e^{ikR}}{4\pi kR} \, d\bar{r}'' \tag{II-2}$$

where $\hat{a}$ is the normal to the aperture pointing to the right (see Figure II-1) and $\bar{E}''$, $\bar{B}''$ are the total aperture fields. These may be written

$$\bar{E} = 2k^2 \int_A \hat{R} \times (\hat{a} \times \bar{E}'') \frac{e^{ikR}}{4\pi kR} \left(\frac{ikR-1}{kR}\right) d\bar{r}'' \tag{II-3}$$

and

$$c\bar{B} = 2k^2 \int_A \hat{R} \times (\hat{a} \times c\bar{B}'') \frac{e^{ikR}}{4\pi kR} \left(\frac{ikR-1}{kR}\right) d\bar{r}'' \tag{II-4}$$

where the notation is as in Appendix I. Since the equations are the same,we will proceed as in Appendix I but using only the electric field.

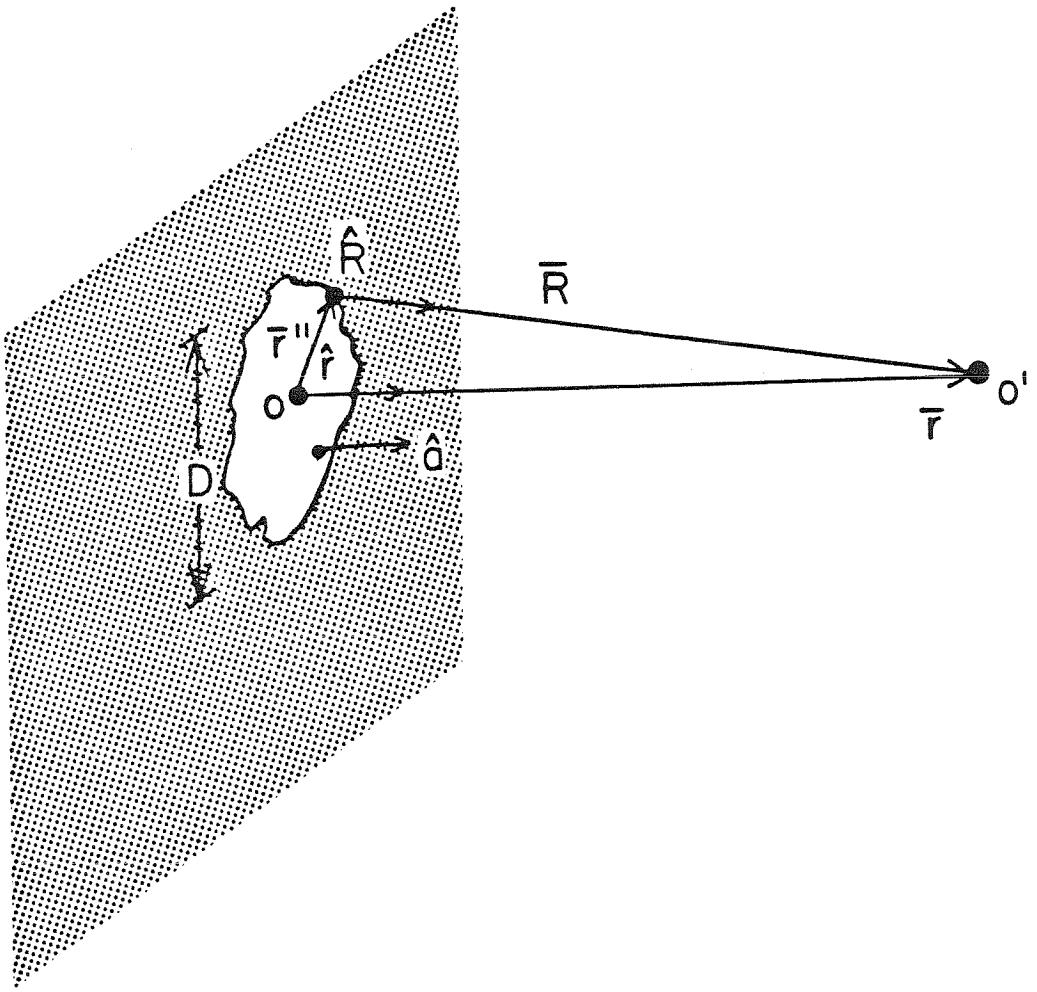

Figure II-1 Aperture Distribution Coordinates

O is the origin of the source frame K

O' is the origin of the observer frame K'
and the point of observation

$\hat{a}$ is the unit vector normal to the aperture

D is the maximum dimension of the aperture

For aperture fields we will only be measuring either the approaching or the receding fields. Using the approximations of Appendix I, we obtain:

$$\hat{\beta}\cdot\frac{\nabla}{k}(\bar{E}\cdot\hat{n})\simeq+is(\bar{E}\cdot\hat{n})+is2k^2\,\frac{e^{ikr}}{4\pi kr}\int\left[+\frac{1}{kr}+\frac{i(\frac{1}{2}k^2r''^2)}{k^2r^2}\right]e^{i\frac{k^2r''^2}{2kr}}(\hat{n}\cdot\bar{E}'')d\bar{r}''e^{-i\omega t} \qquad \text{(II-5)}$$

$$(\bar{E}\cdot\hat{n}) = -\,i2k^2\,\frac{e^{ikr}}{4\pi kr}\int e^{i\frac{k^2r''^2}{2kr}}\,(\hat{n}\cdot\bar{E}'')\,d\bar{r}''\,e^{-i\omega t} \qquad \text{(II-6)}$$

where $\hat{a}=\hat{r}$, $\hat{n}\cdot[\hat{r}\times(\hat{r}\times\bar{E}'')]=-\hat{n}\cdot\bar{E}''$, $\hat{n}\cdot[\hat{r}'\times(\hat{r}\times\bar{E}'')]=0$.

So, now η may be written

$$\eta = s\left(1-\frac{1}{k^2r^2}\,\text{Real}\left\{\frac{\int\frac{1}{2}k^2r''^2\,e^{i\frac{k^2r''^2}{2kr}}\,(\hat{n}\cdot\bar{E}'')\,d\bar{r}''}{\int e^{i\frac{k^2r''^2}{2kr}}\,(\hat{n}\cdot\bar{E}'')\,d\bar{r}''}\right\}\right) \qquad \text{(II-7)}$$

where $s=\begin{cases}+1 \text{ for receding}\\ -1 \text{ for approaching}\end{cases}$

The field functions may similarly be expanded to higher orders in the amplitude showing quadratic amplitude terms in the field itself. This limits the magnitude of the shift as before. A more important approximation, however, is used for most actual aperture field calculations; the total aperture field $\bar{E}''$ will be approximated by the incident aperture field. (This approximation may cause limitations even before higher order amplitude expansions of the fields).

REFERENCES

[1] Ch. Doppler, Über das farbige Licht der Doppelsterne, Abhandlungen der Königlichen Böhmischen Gesellschaft der Wissenschaften, 1843. See also, E. N. Da C. Andrade, Doppler and the Doppler Effect, Endeavor, vol. 18, no. 69, January, 1959.

[2] I. M. Frank, Doppler Effect in a Refractive Medium, J. Phys. U.S.S.R., 2, 49-67 (1943).

[3] K. S. H. Lee, Radiation from an Oscillating Source Moving Through a Dispersive Medium with Particular Reference to the Complex Doppler Effect, Radio Science 3, 1098-1104 (1968).

[4] C. H. Papas, N. Engheta, and A. R. Mickelson, On the Near-Zone Inverse Doppler Effect, IEEE Transactions on Antennas and Propagation, AP-28, pp.519-522, July, 1980.

[5] J. A. Stratton, Electromagnetic Theory, New York, McGraw-Hill 1941, ch.1.

[6] J. D. Dyson, Measurement of Near Fields of Antennas and Scatterers, IEEE Transactions on Antennas and Propagation, AP-21, pp.446-460, July, 1973.

[7] C. H. Papas, Theory of Electromagnetic Wave Propagation, McGraw-Hill Book Co., New York (1965).

[8] M. Born and E. Wolf, Principles of Optics, Oxford, Pergamon Press, Fifth Ed., 1975, Ch. VIII.

[9] IEEE Test Procedure for Antennas, IEEE Transactions on Antennas and Propagation, AP-13, p.437, Jan. 1965.

[10] Radar Handbook, M. Skolnik, editor, New York, McGraw-Hill (1970).

[11] R. C. Hansen, Microwave Scanning Antennas, Vol. I, New York, Academic Press, 1964, Ch. 1.

[12] L. Page, The Electrical Oscillations of a Prolate Spheroid, Paper II, Phys. Rev. 65, 98 (1944).

[13] L. Page, and N. I. Adams, Jr., The Electrical Oscillations of a Prolate Spheroid, Paper I, Phys. Rev. 53, 819 (1938).

[14] C. Flammer, Spheroidal Wave Functions, Stanford, California, Stanford University Press, 1957.

[15] L. J. Chu and J. A. Stratton, Steady-State Solutions of Electromagnetic Field Problems, III. Forced Oscillations of a Prolate Spheroid, J. Appl. Phys. 12, 241 (1941).

[16] M. Schwartz, W. R. Bennett, and S. Stein, Communication Systems and Techniques, New York, McGraw-Hill, 1966. p.232.

[17] J. D. Jackson, Classical Electrodynamics, Second ed., New York, Wiley 1975.